

See discussions, stats, and author profiles for this publication at: <https://www.researchgate.net/publication/229926248>

# Mechanical Properties of Polystyrene/Polyamide 6 Blends Compatibilized with the Ionomer Poly(Styrene-co-sodium Acrylate)

ARTICLE in JOURNAL OF APPLIED POLYMER SCIENCE · MARCH 2004

Impact Factor: 1.77 · DOI: 10.1002/app.20219

---

CITATIONS

13

---

READS

16

5 AUTHORS, INCLUDING:



[Sergio Manuel Nuño-Donlucas](#)

University of Guadalajara

37 PUBLICATIONS 254 CITATIONS

SEE PROFILE



[Jorge E. Puig](#)

University of Guadalajara

193 PUBLICATIONS 2,889 CITATIONS

SEE PROFILE



[Rubén González-Núñez](#)

University of Guadalajara

72 PUBLICATIONS 435 CITATIONS

SEE PROFILE

# Mechanical Properties of Polystyrene/Polyamide 6 Blends Compatibilized with the Ionomer Poly(Styrene-*co*-sodium Acrylate)

M. E. Villarreal, M. Tapia, S. M. Nuño-Donlucas, J. E. Puig, R. González-Núñez

*Departamento de Ingeniería Química, Universidad de Guadalajara, Boul. M. García Barragán No. 1451, Guadalajara, Jal. 44430 Mexico*

Received 24 March 2003; accepted 9 October 2003

**ABSTRACT:** The compatibilizing effect of the ionomer, poly(styrene-*co*-sodium acrylate) (PSSAc), on immiscible blends of polystyrene (PS)/polyamide 6 (PA6) was studied by mechanical tests and scanning electron microscopy. The PSSAc acts as an effective compatibilizer because both the deformation at break (%) obtained by tensile stress-strain tests and the impact rupture energy are larger in blends containing small amounts of PSSAc. The morphologies of

the fractured surfaces produced by tensile stress-strain tests of blends with or without the ionomer confirm that PSSAc increases the interfacial adhesion between PS and PA6 phases. © 2004 Wiley Periodicals, Inc. *J Appl Polym Sci* 92: 2545–2551, 2004

**Key words:** mechanical properties; ionomer; morphology; compatibilizer; blends

## INTRODUCTION

Most polymer blends are immiscible because their miscibility is restricted by a specific set of conditions such as complementary molecular architecture of the parent polymers, molecular weight and molecular weight distribution, temperature, pressure, etc.<sup>1</sup> Most immiscible blends have two-phase morphologies, with weak adhesion between the phases and poor mechanical properties because of unfavorable interactions at the molecular level.<sup>2</sup> However, the compatibilization of these blends improves the mechanical properties and yields better performance.<sup>3</sup>

A compatibilizer is a polymer which, when added to an immiscible polymer mixture, increases the degree of compatibility.<sup>4</sup> A compatibilizer can produce the following three effects: (1) reduce the interfacial tension, thus engendering finer dispersion of one phase in the other<sup>1</sup>; (2) inhibit the growth of the dispersed phase during annealing<sup>5</sup>; and (3) enhance the adhesion between the phases in the solid state facilitating the stress transfer from matrix to dispersed phase and, hence, improve the mechanical properties of the blend.<sup>6</sup>

When graft or block copolymers having segments capable of inducing specific interactions with the

blend components are added to immiscible polymer mixtures, they can act as compatibilizers.<sup>7</sup> In a similar way, small amounts of an ionomer, such as sulfonated polystyrene, improve the mechanical properties of immiscible blends where polystyrene is one of the components.<sup>8–10</sup> In fact, the mechanical properties increase because of the increasing homogeneity of the polymers in the blend.<sup>11–13</sup> When a chemical reaction occurs between the compatibilizer and the components of the blend during the processing, this procedure is commonly referred to as reactive blending.<sup>1</sup> Reactive blending can take place in batch-type melt mixers, but continuous processing equipment such as single- and twin-screw extruders are often preferred.<sup>5</sup>

Polyamide 6 (PA6) is an industrially important polymer because of its low impact strength (particularly below its glass transition temperature); however, its poor processibility and poor dimensional stability have limited its applications.<sup>14</sup> To overcome these drawbacks, PA6 was mixed with a great variety of polymers [polyolefins, polyesters, polyethers, other polyamides, acrylonitrile-butadiene-styrene (ABS) copolymers, polystyrene (PS), styrene copolymers, etc.] without or with a compatibilizer to yield blends with better mechanical, optical, or thermal properties.<sup>15–20</sup>

In this work, we report the mechanical properties (impact strength and tensile tests) and the morphology obtained from the rupture of specimens subjected to tensile tests of PA6/PS blends with or without the ionomer poly(styrene-*co*-sodium acrylate) (PSSAc). Experimental evidence reported here demonstrates that this ionomer is a good compatibilizer for these blends.

Correspondence to: S. M. Nuño-Donlucas (gigio@cencar.udg.mx).

Contract grant sponsor: National Council for Science and Technology of Mexico; contract grant numbers: CONACyT I33982-U; CONACyT 39808-Y.

## EXPERIMENTAL

PA6 (3100 from Celanese, Mexico) is a very hygroscopic polymer; hence, it was kept in an oven for 12 h at 60°C to remove humidity before any testing or mixing. Viscometric measurements of this polymer reveal that  $M_v$  is  $\sim 30,000$  g/mol. PS (HF-777 from Resirene, from Resistol, Lerma, Mexico) with  $M_n = 160,000$  g/mol and  $M_w = 190,000$  g/mol, measured by GPC, was used as received.

The PSSAc was made by emulsion polymerization. The reactions were carried out in a glass reactor for 3 h at 60°C with sodium dodecyl sulfate (99% pure from Tokyo Kasei) as emulsifier ( $m_{SDS}/m_{Monomers} = 0.052$ ) and potassium persulfate (KPS) as initiator ( $m_{KPS}/m_{Monomers} = 0.01$ ). The initial weight ratio of styrene to sodium acrylate was 90/10 w/w. Further details on the synthesis of characterization of this ionomer can be found elsewhere.<sup>21,22</sup>

The blends were prepared in a twin-screw extruder (Leistritz Micro 26 GL/GG-36D) at a screw speed of 100 rpm. Typical temperature settings along the barrel were 230, 235, 240, 245, and 250°C from feed hopper to exit. PS/PA6 blends were made in one step, whereas a two-step process made the PS/PSSAc/PA6 blends: first PSSAc and PS were premixed in the extruder and the resultant mixture was mixed with the PA6, keeping the extruder conditions. The composition studied for the PS/PA6 blends were 10, 20, 30, 70, 80, and 90 vol % PS, whereas those for the PS/PSSAc/PA6 were 10/3/87, 20/3/77, 30/3/67, 67/3/30, 77/3/20, and 87/3/10 in vol %. The binary and ternary blends were prepared at five mixing speeds.

A careful control of the guide-rolls system made it possible to modulate the speed at which the polymer melt was stretched at the end of the extruder. The draw-down ratio (DR) is defined here as

$$DR = \frac{u_1}{u_0}$$

where  $u_1$  is the speed of the take-up device and  $u_0$  is the linear velocity of the extrudate, which was  $\sim 39$  in./min, calculated from the melt densities and the flow rate.<sup>23</sup> Five different DRs ( $=1, 2, 3, 4$ , and  $5$ ) were used to prepare the PS/PA6 blends with or without PSSAc.

Tensile stress-strain tests were carried out at room temperature ( $20 \pm 5^\circ\text{C}$ ) in a UNITED (model Smart-1 SM10-20-30) machine. The probes were prepared by cutting the polymer-ribbon obtained in the extruder according to the ASTM-D638 method. Two crosshead speeds (CS) were used. For blends rich in PS, CS was set at 0.05 in./min, whereas for those rich in PA6, CS was equal to 0.6 in./min.

Charpy impact tests were also done at room temperature in a Gardner machine following the proce-

dure described by the ASTM-D5420 method. All the specimens had dimensions of  $25 \times 75 \times 3 \pm 1$  mm, without a notch.

The morphologies of the surface of the probes created after fracture in tensile tests performed on blends with or without PSSAc were examined in a JEOL JSM-5400 LV scanning electron microscope (SEM) equipped with a quantum superdry detector. Before SEM examination, performed at 15–20 kV, the samples were placed in a Baltec CE SCD004 golden evaporator to electrodeposit a gold layer.

## RESULTS

Tensile tests of PS/PA6 and PS/PSSAc/PA6 blends prepared at DR = 1 are presented in Figure 1. Figure 1(A) depicts the stress-strain plots for PS and PS-rich blends with and without PSSAc. Because of the brittle nature of PS at ambient temperature, the probes of PS and PS-rich blends break at very low deformations. However, as the content of PA6 increases, these blends become slightly ductile. So, the strain at break increases and the rupture stress diminishes for the blends with 10 and 30 vol % PA6 (with or without PSSAc) with respect to those of PS. Also, the strain at break increases with the incorporation of the ionomer. Notice that the blend with 30 vol % PA6 breaks at strains more than twice those of PS and the other PS-rich blends.

The stress-strain responses of blends with high content of PA6 are very different than those of the PS-rich blends, as expected [Fig. 1(B)]. PA6 is a ductile material at room temperature. The stress-strain curve of this polymer shows a necking behavior. After the yield point ( $\sim 40$  MPa), cold drawing before breaking is observed. During cold drawing, the strain and the stress increase; also, the ultimate stress is achieved at  $\sim 45$  MPa. When PS is added to PA6, the necking behavior decreases as the PS content increases. This happens in blends with or without PSSAc. Nevertheless, the strain and the stress increase up to the breaking point in all blends. Blends with PSSAc have larger deformations at break than those without PSSAc. Similar stress-strain responses are observed at other DRs for both PS-rich and PA6-rich blends (not shown).

The Young's moduli of PS, PA6, and their blends, with or without the ionomer, prepared at different DRs, are reported in Table I. The standard deviations in the moduli, also reported in Table I, were estimated from data obtained from at least 15 experiments. The Young's modulus of the PS is high ( $\sim 4000$  MPa); in fact, it is much larger than of those of any of the blends with PA6. This is due to the very small capacity of deformation of PS. Hence, it is necessary to apply higher stresses to initiate the deformation. The Young's moduli of PS-rich blends are smaller than 1580 MPa. Notice that all the PS/PA6 blends contain-

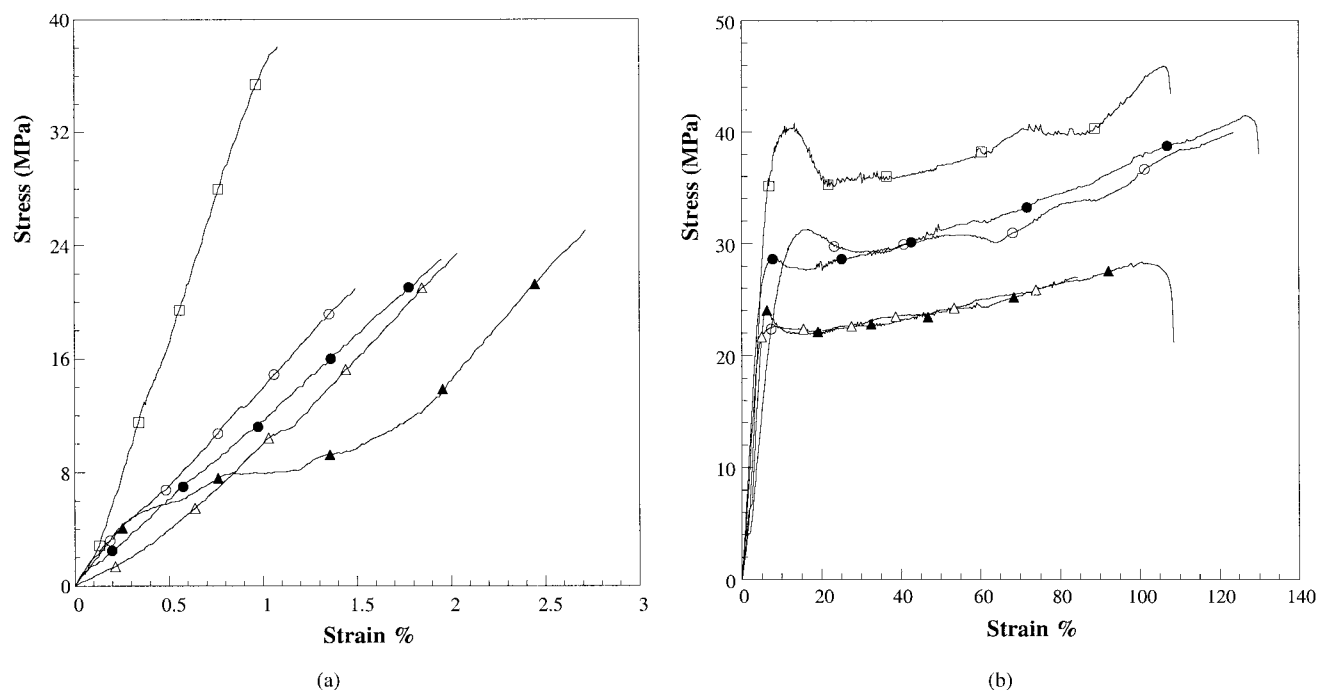


**Figure 1** (a) Tensile stress-strain tests performed at room temperature on PS pure and blends rich in PS. Blend composition is given in vol % PA6. Blends without PSSAc: (□) 0; (○) 10; (△) 30; and blends with PSSAc: (●) 10; (▲) 30. (b) Tensile stress-strain tests carried out at room temperature on PA6 pure and blends rich in PA6. Blend composition is given in vol % PS. Blends without PSSAc: (□) 0; (○) 10; (△) 30; and blends with PSSAc: (●) 10; (▲) 30.

ing PSSAc exhibit slightly larger Young's modulus (Table I).

By contrast, the Young's modulus of PA6 is small ( $\sim 600$  MPa) because of its ductile nature. The Young's modulus of PA6-rich blends without PSSAc is similar to that of PA6 (Table I). However, PA6-rich blends with PSSAc have larger Young's moduli, independently of the composition, than those of blends with-

out the ionomer. It is noteworthy that the Young's modulus of the blend with 20 vol % PS ( $\sim 1200$  MPa) is the largest of all the PA6-rich blends examined. Notice also that the Young's moduli of PA6/PS blends with PSSAc are larger than those of the PA6/PS blends without the compatibilizer at similar compositions at all DRs used in this work. These results were detected either for PS-rich blends or for PA6-rich

**TABLE I**  
Young's Modulus of PA, PA6, and Their Blends Prepared at Different DRs

Composition PS/PSSAc/PA6 (v/v/v%)	Young's modulus (MPa)				
	DR				
	1	2	3	4	5
0/0/100	599 $\pm$ 30	518 $\pm$ 52	492 $\pm$ 44	352 $\pm$ 21	327 $\pm$ 29
10/0/90	388 $\pm$ 25	417 $\pm$ 42	447 $\pm$ 31	429 $\pm$ 43	590 $\pm$ 41
10/3/87	529 $\pm$ 52	482 $\pm$ 26	478 $\pm$ 33	437 $\pm$ 22	434 $\pm$ 30
20/0/80	552 $\pm$ 55	597 $\pm$ 59	696 $\pm$ 66	687 $\pm$ 68	657 $\pm$ 65
20/3/77	1111 $\pm$ 89	664 $\pm$ 20	732 $\pm$ 44	712 $\pm$ 57	677 $\pm$ 47
30/0/70	565 $\pm$ 48	764 $\pm$ 30	724 $\pm$ 72	689 $\pm$ 68	624 $\pm$ 37
30/3/67	735 $\pm$ 73	771 $\pm$ 31	740 $\pm$ 66	692 $\pm$ 21	638 $\pm$ 57
70/0/30	1385 $\pm$ 97	1384 $\pm$ 117	1347 $\pm$ 134	1296 $\pm$ 91	1851 $\pm$ 55
67/3/30	1432 $\pm$ 136	1413 $\pm$ 127	1385 $\pm$ 55	1327 $\pm$ 132	1270 $\pm$ 101
80/0/20	1240 $\pm$ 124	1458 $\pm$ 145	1449 $\pm$ 116	1482 $\pm$ 89	1638 $\pm$ 114
77/3/20	1292 $\pm$ 129	1558 $\pm$ 155	1500 $\pm$ 105	1463 $\pm$ 146	1625 $\pm$ 49
90/0/10	1514 $\pm$ 30	1488 $\pm$ 148	1452 $\pm$ 145	1434 $\pm$ 143	1427 $\pm$ 71
87/3/10	1580 $\pm$ 79	1560 $\pm$ 140	1509 $\pm$ 136	1488 $\pm$ 148	1450 $\pm$ 145
100/0/0	3912 $\pm$ 390	3894 $\pm$ 389	3892 $\pm$ 389	3805 $\pm$ 380	3788 $\pm$ 378

TABLE II  
Deformation at Break of PA6/PS Blends and of the Parent Polymers

Composition PS/PSSAc/PA6 v/v/v %	Deformation at break (%)				
	DR				
	1	2	3	4	5
0/0/100	106 ± 10	130 ± 8	131 ± 11	162 ± 16	120 ± 8
10/0/90	109 ± 11	152 ± 9	163 ± 16	182 ± 16	119 ± 9
10/3/87	133 ± 9	180 ± 12	180 ± 14	184 ± 9	148 ± 7
20/0/80	97 ± 9	142 ± 13	146 ± 14	165 ± 13	162 ± 9
20/3/77	135 ± 13	145 ± 13	168 ± 11	171 ± 15	165 ± 11
30/0/70	87 ± 5	125 ± 7	144 ± 14	151 ± 9	144 ± 14
30/3/67	106 ± 10	127 ± 5	154 ± 12	163 ± 16	159 ± 5
70/0/30	2.1 ± 0.2	2.3 ± 0.2	2.3 ± 0.2	2.1 ± 0.2	1.9 ± 0.2
67/3/30	2.6 ± 0.2	2.5 ± 0.2	2.4 ± 0.2	2.2 ± 0.2	2.1 ± 0.2
80/0/20	2.4 ± 0.2	2.2 ± 0.1	2.2 ± 0.1	2.0 ± 0.1	1.7 ± 0.1
77/3/20	2.5 ± 0.2	2.3 ± 0.2	2.2 ± 0.2	2.1 ± 0.1	2.1 ± 0.2
90/0/10	2.3 ± 0.2	1.9 ± 0.1	1.6 ± 0.1	1.7 ± 0.1	1.8 ± 0.1
87/3/10	2.4 ± 0.1	2.3 ± 0.1	1.8 ± 0.1	1.7 ± 0.1	1.8 ± 0.1
100/0/0	1.1 ± 0.1	1.1 ± 0.1	1.0 ± 0.1	0.9 ± 0.1	0.7 ± 0.1

All these polymers were prepared at different DRs.

blends. So, it seems that the presence of PSSAc modifies the characteristics of the PA6-PS interface, improving the transfer of stress between the ductile PA6 and the brittle PS domains.

The deformations at break (in %) of the parent polymers and their blends with or without the compatibilizer, made at different DRs, are reported in Table II. Again, the standard deviations were calculated from data obtained from at least 15 experiments. PS breaks at very low deformations ( $\sim 1\%$ ), whereas PA6 exhibits very large deformations at break ( $>100\%$ ). Addition of PA6 increases the deformation at break of the PS-rich blends. Notice that the incorporation of PSSAc has little effect on the deformation at break in all the PS-rich blends (Table II). At the other extreme, PA6 exhibits a large deformation at break because of its ductile nature. Addition of PS, as expected, decreases

the deformation at break of the PA6-rich blends. However, with the incorporation of PSSAc, the deformations at break are larger than those of blends without PSSAc, and they are even larger than the deformation at break of PA6 (Table II). An explanation for this behavior is that PSSAc is located mostly at the interface of PA6/PS blends acting as an effective compatibilizer. This behavior is mainly detected for PA6-rich blends. Similar results were reported for blends of PA6 and polyethylene when a graft copolymer of low-density polyethylene and butyl acrylate was added for compatibilization.<sup>14</sup>

Charpy impact tests for blends with or without PSSAc made at different DRs are presented in Figure 2. Because the polymer-ribbon probes prepared by extrusion had different thicknesses, the break energy was divided by the thickness to normalize the results.

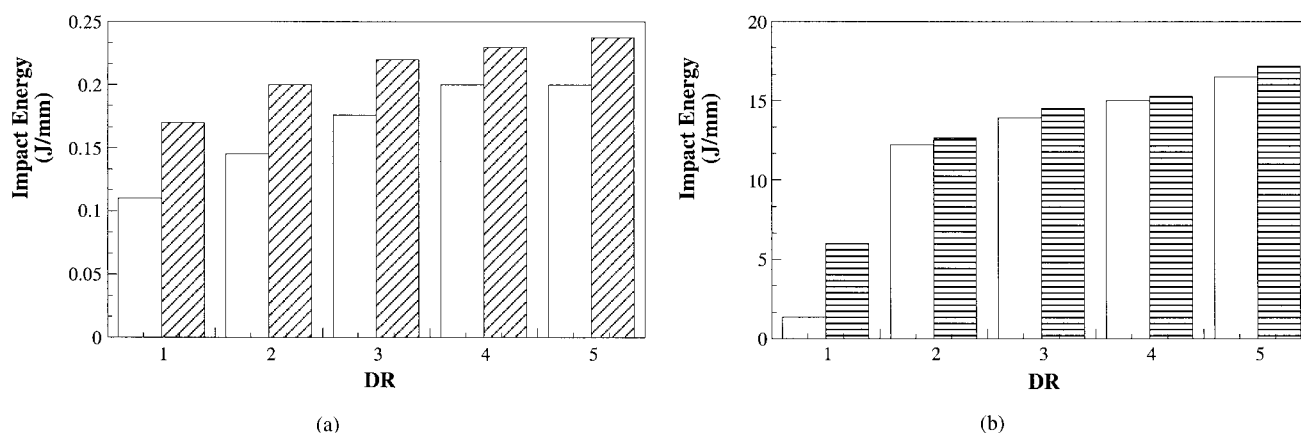


**Figure 2** (a) Charpy impact test of PS-rich blends with (▨) and without (□) PSSAc prepared at different DRs. The compositions of all these blends were 20 vol % PA6. (b) Charpy impact test of PA6-rich blends with (▨) and without (□) PSSAc prepared at different DRs. These blends contain 20 vol % PS.

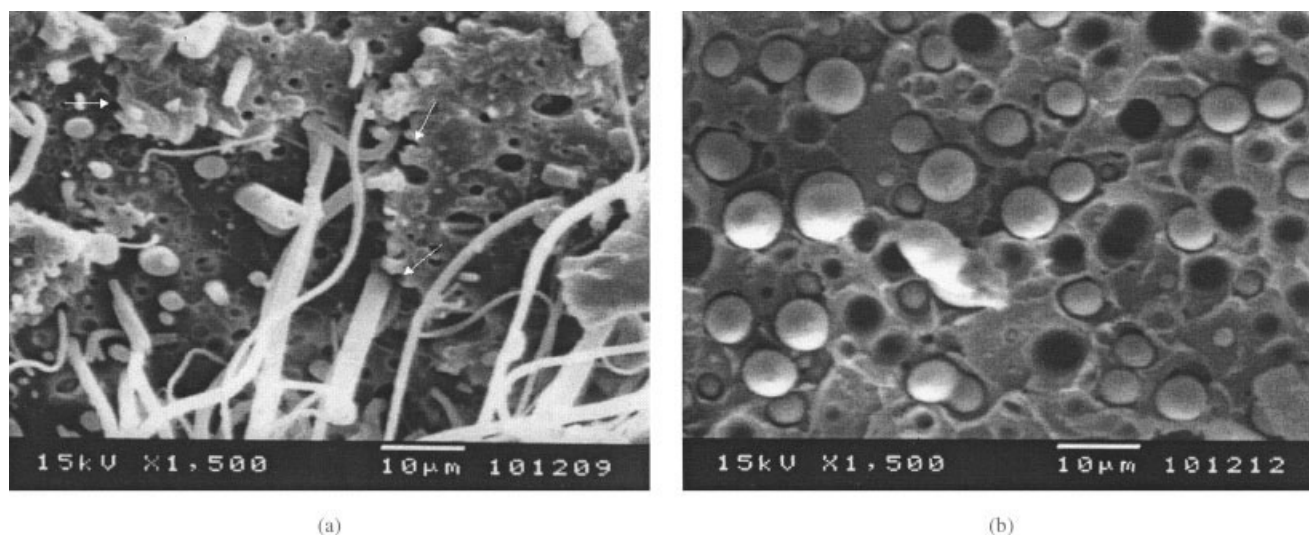


**Figure 3** (a) SEM photograph of the fractured surface after tensile stress-strain test performed on the PS/PA6 blend with 30 vol % PA6. (b) SEM photograph of the fractured surface after tensile stress-strain test performed on the PS/PSSAc/PA6 blend with 30 vol % PA6.

The PA6/PS blends with PSSAc absorb more energy until breaking than those without the ionomer; also, the impact energy increases in both PS-rich [Fig. 2(A)] and PA6-rich [Fig. 2(B)] samples as the DR increases. As expected, PA6-rich samples without or with the ionomer stand higher impact energies than the PS-rich samples [cf. Fig. 2(A, B)]. Because the morphology of the polymer-ribbon changes as the DR increases,<sup>24</sup> the modifications in the morphology can largely influence the capacity of PA6/PS blends to absorb the energy of the mechanical impact.

SEM photographs of the fractured surfaces obtained by tensile tests in blends containing 30 vol % PA6 with or without PSSAc show very different morphologies (Fig. 3). In both cases, PS forms the continuous phase and PA6 forms the dispersed phase. This was proven by using selective solvents: the blend dissolved with toluene, which is a good solvent for PS, whereas the blend maintained its form with formic acid, which is a good solvent for PA6.<sup>25</sup> The fractured surface of the blend without PSSAc exhibits a two-phase structure with filaments coming out of the dispersed phase [Fig. 3(A)]. Inasmuch as PA6 is a semicrystalline and ductile polymer and PS is brittle, the poor interfacial adhesion between these two polymers evidently caused the elongation of the ductile PA6 domains when the fractured surfaces were pulled apart. Peterlin proposed that the cold drawing in ductile semicrystalline polymers occurs in three stages, where a fibrous structure is created at the final stage.<sup>26</sup> Hence, the fibrous structures (filaments) observed in Figure 3(A) correspond to the final stage of the Peterlin model. PS, on the other hand, being a brittle material, caused the formation of layers with sharp borders in the continuous domains of the fractured surfaces [see arrows in Fig. 3(A)].

In contrast, when a small amount of PSSAc is added to the blend containing the same vol % of PA6, the morphology of the fractured surface changes substantially; now a two-phase structure with no filaments is observed [Fig. 3(B)]. Here, the PA6 phase forms spheroidal microregions dispersed in the PS matrix. Hence, to explain the differences in morphology, we proposed that the presence of the PSSAc at the interface and the chemical reaction taking place with PA6, as demonstrated by us elsewhere,<sup>25</sup> strongly enhances the interfacial adhesion between the two polymers in such a way that no filaments of PA6 form when the fractured surfaces are pulled apart.

The fractured surfaces of PA6-rich blends (20 vol % PS) with or without PSSAc are displayed in Figure 4. Notice that they are completely different than those of the PS-rich blends (cf. Figs. 3 and 4). Now, in both micrographs, fiber-like structures are observed coming out of the surface together with small spheroidal domains at the surface. Selective solvent extraction reveals that PA6 forms the matrix in these blends.<sup>25</sup> Hence, when the surfaces are pulling apart after fracture, strong rearrangements occurs in the PA6 matrix and fibrillation is achieved under cold-drawing conditions.<sup>27</sup> Notice, however, that the fibers are shorter and thinner in the fractured surface of the blend containing PSSAc [Fig. 4(A)] than in the surface of blend without PSSAc [Fig. 4(B)] (notice that the magnification in both pictures is the same). Also, the PS spheroidal domains [indicated by arrows in Fig. 4(A, B)] are much smaller in the sample containing the ionomer. The compatibilization influence of PSSAc is clear by the minor size of the PS spheroidal domains and the smaller length and thickness of the fibers.

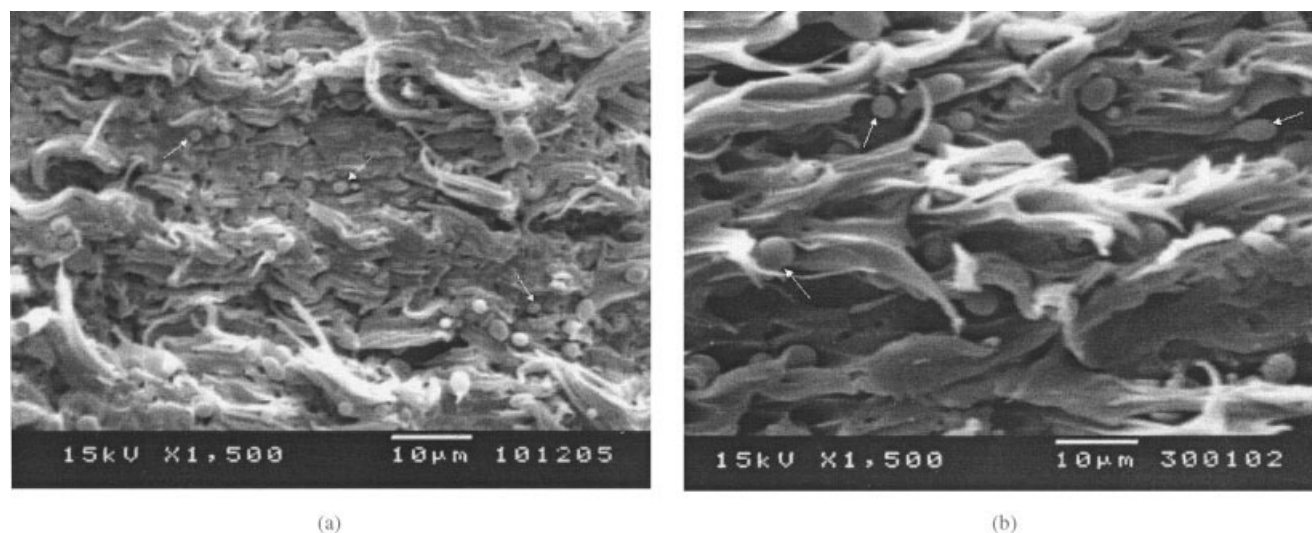


**Figure 4** (a) SEM photograph of the fractured surface of PS/PSSAc/PA6 blend with 20 vol % PS. (b) SEM photograph of the fractured surface of PS/PA6 blend with 20 vol % PS.

## DISCUSSION AND CONCLUSIONS

PS and PA6 are immiscible at all proportions.<sup>1</sup> Therefore, the interfacial adhesion between these polymers is weak. Because the mechanical properties of PS/PA6 blends are poor, it is necessary to add a compatibilizer to improve these and other properties.

PSSAc is an ionomer with about 95 wt % PS that has acid (COOH) and salt (COONa) groups, which can interact chemically or physically with groups of other polymers.<sup>22</sup> Rodríguez-Ríos et al. reported that PSSAc has the capacity to reduce the size of the disperse phase in blends of PS and PA6 because a chemical reaction occurs between the carboxylic groups of PS-SAc and the amine groups of PA6.<sup>25</sup> They proposed a reaction scheme where the amine terminal groups of PA6 chemically bind to the carboxylic groups of PS-SAc, producing water molecules as a reaction product. This reaction is carried out during the mixing process by melting at 250°C in an internal chamber mixer.

The results of tensile stress-strain (Fig. 1) and impact tests (Fig. 2) suggest that the chemical interactions improve the mechanical behavior of these blends. The stress-strain curves of PS-rich blends reveal a classical behavior of hard and brittle materials with very little strain deformation and high stress until breaking [Fig. 1(A)].<sup>27</sup> On the other hand, the stress-strain curves of the PA6-rich blend show a yield point, after necking with cold drawing behavior [Fig. 1(B)]. Similar stress-strain curves were reported elsewhere for blends where PA6 is the main component.<sup>7,14</sup> The deformations at break of blends with the ionomer are larger than those of the blends without the compatibilizer at all compositions (Table II). This result is crucial to elucidate the role of the PSSAc in the improvement of the mechanical properties of these

blends. The deformation at break is very sensitive to interfacial adhesion between polymer phases in blends.<sup>28–30</sup> Then, because of its large polystyrene content and its capacity to react chemically with amine groups of PA6 (because it contains COOH and COONa groups), it is likely that PSSAc augments the interpenetration between the PS and PA6 phases and enhances the interfacial adhesion between these phases. Although the processing conditions to prepare binary and ternary blends changed (DR was varied from 1 to 5) and, therefore, the morphology in the ribbon-polymer may be modified thus affecting the mechanical properties, the deformation at break is always larger in the blends containing PSSAc (Table II). This suggests that this mechanical response was not determined by the preparation procedure but mainly by the presence of PSSAc. Charpy impact tests also demonstrate that the impact energy of all blends with PSSAc is higher than in blends without PSSAc (Fig. 2). Because the impact test reflects the toughness of a polymer,<sup>27</sup> these results indicate that the toughness of the ternary blends increases because the capacity to absorb impact increases. Then, because of the incorporation of PSSAc at the interface between PS and PA6 domains, the transfer of the strain between the brittle PS and the ductile PA6 augments. Moreover, that the Young's moduli of the blends containing PSSAc, especially those of PA6-rich blends, are larger than those of the blends that do not contain the ionomer (Table I) demonstrate that PSSAc is acting as a compatibilizer.

The SEM micrographs of the fractured surfaces of the blends with and without the ionomer made by tensile stress-strain tests show dramatic differences. Although fibrous structures originated by cold draw-

ing of PA6 can be detected in the fractured surface of the PS-rich blend without the ionomer [Fig. 3(A)], the fractured surface of the PS/PSSAc/PA6 blend shows the classical two-phase structure detected in many immiscible blends,<sup>28</sup> where the component in minor quantity form spheroid microregions dispersed without order in the matrix [Fig. 3(B)]. Also, the fractured surfaces of the PA6-rich blends show important differences depending on whether the ionomer is present or not (Fig. 4). The differences in morphology suggest that PSSAc increases the interfacial adhesion in such a way that the contributions of PA6 (ductile polymer) and PS (brittle polymer) to the fractured surfaces could not be appreciated. Rodríguez-Ríos et al. reported a very similar morphology to that shown in Figure 3(B) for PS/PSSAc/PA6 blends, but with a difference that the fractured surface was created by immersing samples of PS-rich blends in liquid nitrogen.<sup>25</sup> Therefore, the cold drawing process was not carried out.

In summary, we have shown that PSSAc acts as a compatibilizer in immiscible mixtures of PS and PA6. The deformation at break and the impact energy in blends with PSSAc are larger than in blends without this ionomer, even when the preparation conditions were varied (Table II and Fig. 2). SEM photographs of the fractured surface of PS/PA6 blends (Figs. 3 and 4) also confirm the compatibilization effect of PSSAc in these blends, regardless of which, PS or PA6, is the main component.

The National Council for Science and Technology of Mexico (CONACyT I33982-U and CONACyT 39808-Y) supported this research. M. E. Villarreal Salazar acknowledges the scholarship provided by CONACyT.

## References

1. Utracki, L. A. *Commercial Polymer Blends*; Chapman & Hall: London, 1998.
2. Kim, D. H.; Park, K. Y.; Kim, J. Y.; Suh, K. D. *J Appl Polym Sci* 2000, 78, 1017.
3. Park, S. H.; Park, K. Y.; Suh, K. D. *J Polym Sci, Part B: Polym Phys* 1998, 36, 447.
4. Datta, S.; Lohse, D. J. *Polymeric Compatibilizers: Uses and Benefits in Polymer Blends*; Hanser Publishers: Munich, 1996.
5. Bonner, J. G.; Hope, P. S. *Polymer Blends and Alloys*; Folkes, M. J.; Hope, P. S., Eds.; Blackie Academic & Professional: London, 1993; Chapter 3.
6. Barlow, J. W.; Paul, D. R. *Polym Eng Sci* 1984, 24, 525.
7. Sathe, S. N.; Devi, S.; Rao, G. S. S.; Rao, K. V. *J Appl Polym Sci* 1996, 61, 97.
8. Bellinger, M.; Sauer, J. A.; Hara, M. *Macromolecules* 1994, 27, 6147.
9. Hara, M.; Bellinger, M.; Sauer, J. A. *Polym Int* 1991, 26, 137.
10. Hara, M.; Sauer, J. A. *JMS-Rev Macromol Chem Phys* 1998, C38 (2), 327.
11. Ide, F.; Hasegawa, A. *J Appl Polym Sci* 1974, 18, 963.
12. Martuscelli, E.; Riva, F.; Sellitti, C.; Silvestre, L. *Polymer* 1985, 26, 270.
13. Cimino, S.; Coppola, F.; D'Orazio, L.; Greco, R.; Maglio, G.; Malinconico, M.; Mancarella, C.; Martuscelli, E.; Ragosta, G. *Polymer* 1986, 27, 1874.
14. Raval, H.; Devi, S.; Singh, Y. P.; Mehta, M. H. *Polymer* 1991, 32 (3), 493.
15. Curto, D.; Valenza, A.; La Mantia, F. P. *J Appl Polym Sci* 1990, 39, 865.
16. Yasue, K.; Marutani, T.; Fukushima, Y.; Ida, T. (to Stamicarbon) U.S. Pat. 5,043, 385, 1991.
17. Mussig, B.; Meyer, R.-V.; Brassat, B.; Dhein, R. (to Bayer) U.S. Pat. 4,820,771, 1989.
18. Khanna, Y. P.; Turi, E. A.; Aharoni, S. M.; Largman, T. (to Allied) U.S. Pat. 4,417, 032, 1983.
19. Majumdar, B.; Keskkula, H.; Paul, D. R. *Prepr ACS Div of Polym Chem* 1993, 34, 844.
20. Bilech, H. A.; Cooper, E. (to Polysar) U.S. Pat. 5,032,644, 1991.
21. Nuño-Donlucas, S.; Rhoton, A. I.; Corona-Galván, S.; Puig, J. E.; Kaler, E. W. *Polym Bull* 1993, 30, 207.
22. Nuño-Donlucas, S. M.; Díaz-Nájera, L. M.; González-Núñez, R.; Martínez-Rico, M. A.; Puig, J. E. *J Appl Polym Sci* 1997, 66 (5), 879.
23. González-Núñez, R.; Arellano, M.; Moscoso, F. J.; González-Romero, V. M.; Favis, B. D. *Polymer* 2001, 42, 5485.
24. González-Núñez, R.; Favis, B. D.; Carreu, P. J. *Polym Eng Sci* 1993, 33 (13), 851.
25. Rodríguez-Ríos, H.; Nuño-Donlucas, S. M.; Puig, J. E.; González-Núñez, R.; Schulz, P. C. *J Appl Polym Sci* 2004, 91, 1736.
26. Peterlin, A. *J Mater Sci* 1971, 6, 490.
27. Nielsen, L. E.; Landel, R. F. *Mechanical Properties of Polymers and Composites*, 2nd ed.; Marcel Dekker: New York, 1994.
28. Laurienzo, P.; Immirzi, B.; Malinconico, M. *Macromol Mater Eng* 2001, 286, 248.
29. Paul, D. R. *Polymer Blends*; Paul, D. R.; Newman, S., Eds.; Academic Press: New York, Vol. 2, 1978.
30. Akkapeddi, M. K.; Van Buskirk, B. *Polym Mater Sci Eng* 1992, 67, 317.